

Analysis of Optimum Temperature and Calcination Time in the Production of CaO Using Seashells Waste as CaCO₃ Source

Sarah Dampang¹, Endah Purwanti², Fredina Destyorini³, Setyo Budi Kurniawan⁴, Siti Rozaimah Sheikh Abdullah⁴, Muhammad Fauzul Imron^{5*}

¹ Study Program of Chemical Engineering, Faculty of Engineering, Universitas Singaperbangsa Karawang, 41361 Karawang, Jawa Barat, Indonesia

² Study Program of Environmental Engineering, Faculty of Engineering, Universitas Singaperbangsa Karawang, 41361 Karawang, Jawa Barat, Indonesia

³ Research Center for Physics, Indonesian Institute of Sciences (LIPI), Jakarta 12710, Indonesia

⁴ Department of Chemical and Process Engineering, Faculty of Engineering and Built Environment, Universiti Kebangsaan Malaysia, 43600 UKM Bangi, Selangor, Malaysia

⁵ Study Program of Environmental Engineering, Department of Biology, Faculty of Science and Technology, Universitas Airlangga, Kampus C UNAIR, Jalan Mulyorejo, Surabaya 60115, Indonesia

* Corresponding author's email: fauzul.01@gmail.com

ABSTRACT

Seashells waste is abundant in coastal area, especially in the locations where fisheries are a major occupation. This abundant resource of seashells opens a new opportunity further utilization. Seashells waste is a source of CaCO₃, which may be converted into CaO via the calcination process. This study analyzed the characteristics of the CaO produced via calcination process at different temperature and calcination time. The calcination process was carried out at a temperature of 800°C, 900°C, and 1000°C with variation of 2, 3, and 4 hours in time. The Fourier transform infrared spectroscopy (FTIR) result showed that the spectrum of 2513 cm⁻¹ as an indication of the C-H group containing CaO appearing after calcination. The FTIR results suggest that the calcination time did not gave major alteration to the functional groups. The results of X-ray diffraction (XRD) analysis showed that CaO laid at the angle of 58.1° and 64.6°. Scanning Electron Microscopy–Energy Dispersive X-Ray Spectroscopy (SEM-EDS) results showed that the most significant compositional outcome after the calcination process was Ca and O at all temperatures and calcination times. All calcined seashells showed rough surface and irregular shape particles. The result of a Thermogravimetric analysis (TGA) suggested that the highest mass alteration occurred at a temperature of 800°C with 78 mins of calcination time.

Keywords: characterization; conversion; environment; FTIR; SEM-EDX; TGA

INTRODUCTION

Seashells waste is considered to be abundant in coastal area, especially in the location where most of the population works in fisheries (Kurniawan and Imron, 2019a; Morris et al., 2019). Seashells waste can be converted into useful and economically viable products (Imron et al., 2020; Kurniawan and Imron, 2019b; Mo et al., 2018). The conversion of seashell waste into new minerals for sustainable cementitious materials is a

substitute and additional mineral fillers in cement has also been proven to be suitable (Morris et al., 2019; Wang et al., 2019; Wulandari et al., 2021). Besides, seashell waste can also become a support material for the photocatalytic synthesis process (Kurniawan et al., 2020; Wang et al., 2020).

Several studies have found that the dominant seashell component is CaCO₃ (approx. 96%), called calcite, and small amounts of other minerals (Yoon et al., 2003). Another research also mentions that seashells consist of 98% calcium

carbonate, and when calcined above 700°C, it turns into CaO (Sirisomboonchai et al., 2015). The benefit of seashells as a raw material in the production of CaO is a carrier for heterogeneous catalysts that can reduce the biodiesel production costs as well as the amount of seashells waste (Hadiyanto et al., 2016). Seashells have characteristics of 98% CaCO₃, 0.79% MgCO₃, and 0.15% SrCO₃ (Sirisomboonchai et al., 2015). There is also a high Ca content in the seashell waste as a source of CO₂ absorption (Huang et al., 2018).

According to Kaplan (1998), the seashells consist mostly of CaCO₃ (95–99% CaCO₃), but when heated to a specific temperature, it produced a single metal oxide CaO. Referring to Kwon et al. (2004), seashell waste is an effective reagent that can remove phosphorus from wastewater. Calcination temperature and time played important role in the characteristics of the produced compounds (Ramasamy et al., 2016). When heated to temperatures higher than 750–800°C, the seashells can turn into good calcium oxide (Nordin et al., 2015). Through a thermal decomposition process known as calcination, the CaCO₃ becomes CaO used in industry and everyday practices such as water and sewage treatment, glass production, construction materials, agriculture, and others (Lin et al., 2011; Mohamed et al., 2012).

Seashell waste is abundant in Tanjung Baru Beach, Karawang, Jawa barat, Indonesia. The utilization of this waste has not been explored yet, especially as a calcium carbonate source (CaCO₃) to produce solid CaO which may be utilized further. This study was aimed at utilizing seashell waste as the source of calcium carbonate to produce solid CaO at various temperatures and period of calcination as well as to characterize the produced compounds. This research was expected that the obtained CaO will be environmentally friendly and can be used in various fields.

MATERIALS AND METHODS

Source and pretreatment of seashells waste

The seashells were taken from Tanjung Baru, Karawang, Jawa Barat, Indonesia, about 38 km from the University of Singaperbangsa Karawang. The seashells were sorted into large ones and used in the research. The obtained seashells were then cleaned by using tap water and dried under

the sun (Kadir et al., 2020; Wang et al., 2019). After drying, the process was repeated by using NaOH 10% (Pudak Scientific, Indonesia) and Aquadest (Shagufta Laboratory, Indonesia) to remove the impurities that still clung to the shells (Tang et al., 2011). After the double cleansing, seashells were laid under the sun until dry (Titah et al., 2018a). The cleaned and dried seashells were ground to obtain the powder form. The seashells powder were then dried in a DHG 9053A oven (Zenithlab, USA) for twenty-four hours at 105°C (Kaewdaeng et al., 2017). The oven samples were sieved with a size of 100 mesh to obtain homogeneous powder. The homogenous powder was then subjected to the calcination process (Abutu et al., 2019).

Analysis of the optimum temperature and calcination time for CaO production

In the calcination process, total of 20 grams of powder were stored in a desiccator to obtain stable balance (Almansoory et al., 2020; Purwanti et al., 2017). The seashells powder were calcined using an electric furnace (Neytech Vulcan, USA) with the temperature variation of 800°C with a calcination time of 2–4 hours (Kouzu and Hidaka, 2012), 900°C with a calcination time of 2–4 hours (Boey et al., 2011), and 1000°C with a calcination time of 2–4 hours (Sirisomboonchai et al., 2015).

Characterization of produced compounds after calcination

The characterization and analysis of the sample were carried out based on the functional group analysis using the Fourier Transform Infrared Spectroscopy (FT-IR) Model Prestige 21 (Shimadzu, Japan) (Ajao et al., 2018). The crystallinity analysis was conducted using X-ray Diffraction (XRD) MiniFlex Type (Rigaku, Japan) (2θ range of 0–90° at a scanning speed of 1° min⁻¹) (Wang et al., 2021). The surface morphology and composition of compounds were analyzed using Scanning Electron Microscopy – Energy Dispersive X-Ray Spectroscopy (SEM-EDS) Model JSM-IT300LV (Jeol, Japan) (Titah et al., 2019, 2018b). The study of mass changes as a function of temperature or time under controlled conditions was conducted using Thermogravimetric analysis (TGA) model TAPT-1600 (Linseis, Germany), with N₂ gas flow conditions at 4 liters/hour, 1 gr sample,

room temperature 100–1200°C, temperature flow 10°C min⁻¹ (default) (Saleh et al., 2017).

RESULTS AND DISCUSSION

Characterization using FTIR

On the basis of Figure 1, the IR spectrum of seashell powder before and after calcined showed different transmittance and functional group. Several different peaks appeared after calcination. Some peaks did not appear in the uptake of seashell powder before calcination but appeared on the spectrum after calcination. Before calcination, an absorption band appears at the wave number 3429.43 cm⁻¹. After calcination, several wavenumbers around 3400 cm⁻¹ belong to the O-H group vibrational absorption bands from Ca(OH)₂ due to forming the O-H group attached to the calcium atom (Suryaputra et al., 2013).

In the seashell powder, before calcination, the IR spectrum shows the absorption band change at the wavenumber of 1475.54 cm⁻¹ and a sharp peak appearing. In contrast, the peaks are widened after calcination. The wavenumber belongs to the C-O vibration in the carbonate functional group of CaCO₃. The absorption band on the shell powder after calcination at several time variations in general. The absorption pattern was not much different, even though there were differences in the absorption intensity. However, the temperature variation was sufficient to affect the IR spectrum results, shown by the widening of the spectrum peaks by the increasing of the calcination temperature (Brites et al., 2018). This indication is pointing that CaCO₃ has changed into CaO due to the heating process.

The CaO was detected at the absorption band of 2513.25 cm⁻¹ which is a characteristic of the peak of the C-H functional group. The samples that have CaO showed the C-H stretching vibrations. It can also be seen that the presence of CaO was indicated by the appearance of the absorption band at a wavelength of 709.80 cm⁻¹. This absorption band is a fingerprint that indicates the presence of CaO bonds, as mentioned by Raizada et al. (2017). The FTIR results indicated that the calcination time did not affect the functional group of seashells. On the other hand, the increasing of calcination temperature showed an alteration to the IR spectrum.

Characterization using XRD

Figure 2 showed the XRD characterization patterns of seashells, before and after the calcination process. The results displayed the

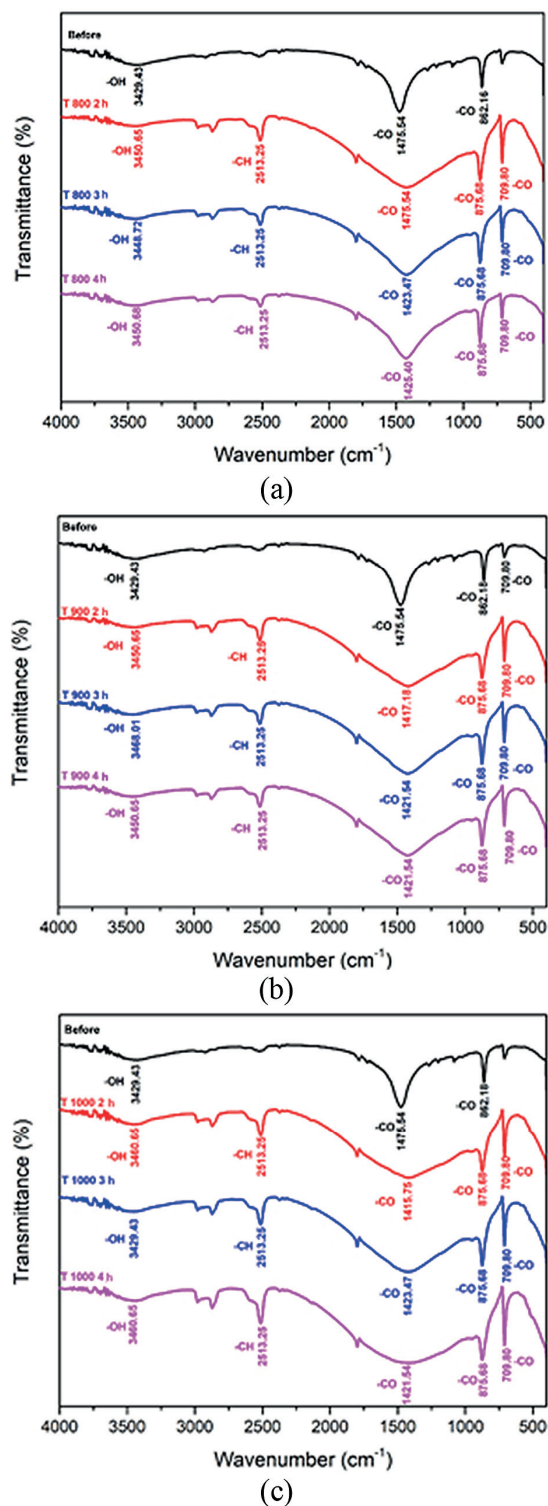


Figure 1. FTIR result for compounds before and after calcination process at (a) 800°C, (b) 900°C, and (c) 1000°C

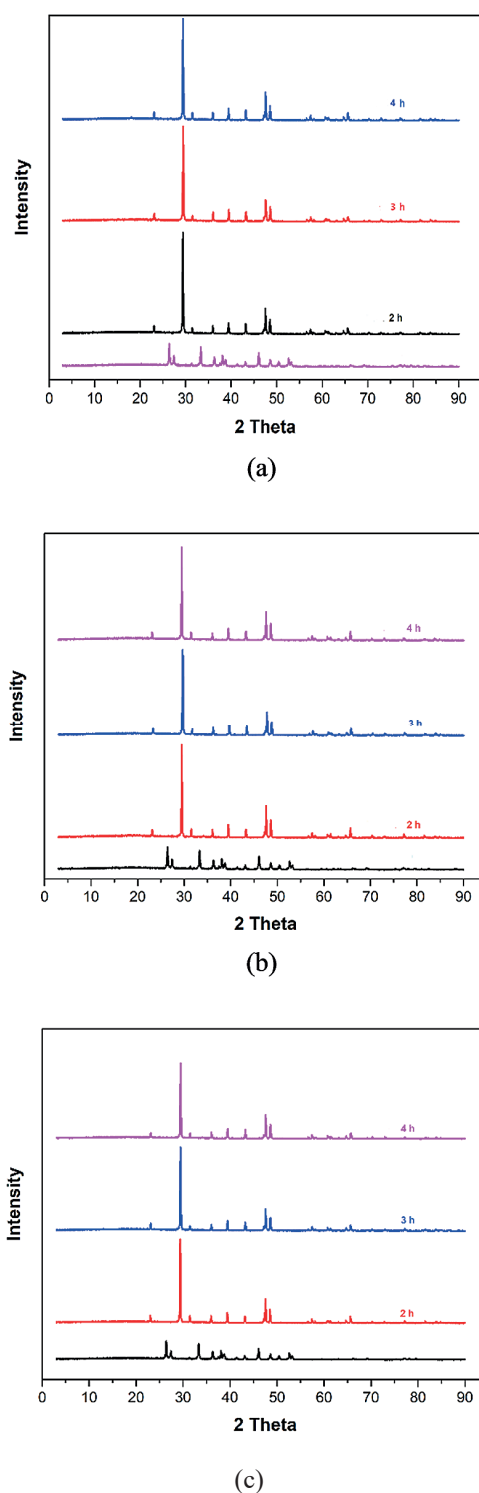


Figure 2. XRD result for compounds before and after calcination process at (a) 800°C, (b) 900°C, and (c) 1000°C

calcium contained in the shells is calcium carbonate (CaCO_3). These XRD peaks were adjusted to the Joint Committee on Power Diffraction Standards (JCPDS) for CaCO_3 and CaO (Nakatani et al., 2009). In the CaCO_3 phase, the highest peaks are at angles of 29.4°, 39.4°, 43.2°, 47.5° and

48.5°. Meanwhile, the CaO phase with a minimal intensity is at the angle of 58.1° and 64.6°. The appearance of the CaO phase was obtained because several CaCO_3 compounds have changed phase after the calcination process (Berent et al., 2019). The XRD results indicated that the variation of temperature and calcination time did not have a significant effect because the obtained peaks were almost the same.

Characterization using SEM-EDX

Figure 3 show the result of surface morphology of seashell powder, before and after the calcination process. The most dominant elements were C (18.43%), O (52.07%), and Ca (27.86%) for the seashells before calcination (Figure 3a). The features of C, Na, Al, Si, Fe, and Cu are minimal due to the heating process (calcination). In turn, for the O and Ca elements in the seashells calcined at 800°C, the obtained composition of O was 56.97% and Ca was 43.03% (Figure 3b). The temperature of 900°C gave a similar composition of O (62.71%) and Ca (37.29%) (Figure 3c) and the temperature of 1000°C also showed a similar content of O (63.56%) and Ca (36.44%) (Figure 3d). Meanwhile, in the research conducted by Suryaputra et al. (2013), the calcined seashells at 1000°C had higher different composition of O (50.14%) and Ca (49.86). The different composition occurred due to the different initial materials used for the research (Abutu et al., 2019; Wang et al., 2019). In the SEM analysis, the seashells calcined at 800°C, 900°C, and 1000°C showed a rough surface, and irregular shaped particles gathered into bulk with an individual diameter of 1 μm .

Characterization using TGA analysis

The TGA analysis results showed a significant change in mass begins to occur around temperatures of 780°C. This mass decrease indicates the decomposition of CaCO_3 to CaO due to the release of CO_2 compounds (Bazargan et al., 2015). The temperature of 800.5°C and calcination period of 78 minutes gave the highest mass changes for the seashells. After passing the temperature around 900°C, it appears that the mass change curve was relatively constant. The curve indicates that above temperatures of 900°C to 1200°C, there is no change in the CaO compound (Dümichen et al., 2015).

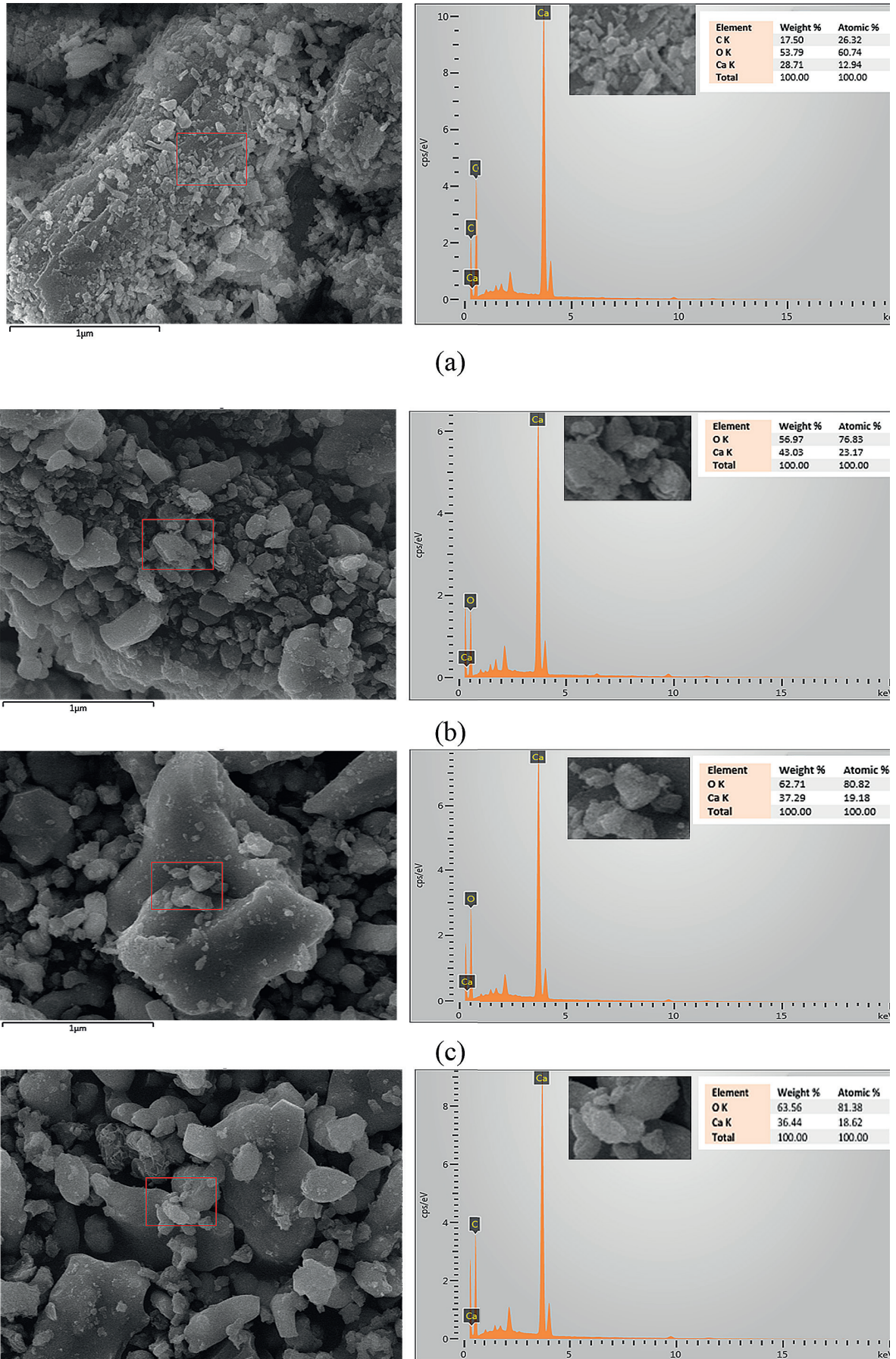


Figure 3. SEM-EDX result for compounds (a) before calcination and after calcination process at (b) 800°C, (c) 900°C, (d) 1000°C

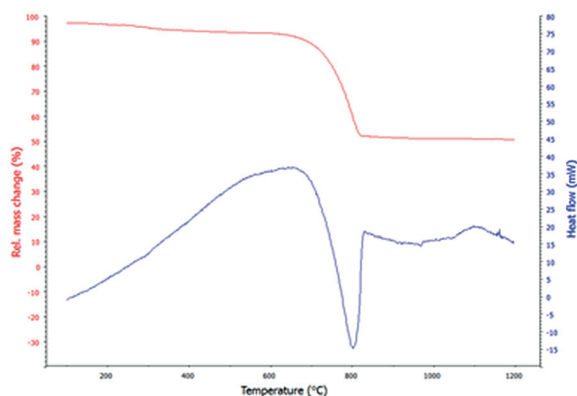


Figure 4. TGA Analysis of calcination process under different temperature

CONCLUSIONS

FTIR analysis of calcined seashells with variations in time (2–4 hours) and temperature (800–1000°C) produced a similar spectrum (2513.25 cm^{-1}) which belongs to the characteristic of the peaks of the C-H group containing calcium oxide (CaO). The absorption band appearance at a wavelength of 709.80 cm^{-1} was a fingerprint indicating the presence of CaO bonds. The FTIR spectrum indicated that the calcination time did not affect the production of CaO. The XRD characterization showed a similar pattern, indicating that the calcination time and temperature did not affect the cementitious component. The SEM-EDX analysis showed that the higher the calcination temperature, the lower the calcium content, with similar irregular particles. The results of the TGA analysis showed that after passing the temperatures of 900°C the mass change curve seemed to be relatively constant, with 800.5°C giving the highest mass differences.

REFERENCES

1. Abutu, J., Lawal, S.A., Ndaliman, M.B., Lafia-Araga, R.A., Abdulrahman, A.S., 2019. Effects of Particle Size Distribution on the Properties of Natural-Based Composite. *Int. J. Eng. Mater. Manuf.* 4, 170–177. <https://doi.org/10.26776/ijemm.04.04.2019.05>
2. Ajao, V., Bruning, H., Rijnaarts, H., Temmink, H., 2018. Natural flocculants from fresh and saline wastewater: Comparative properties and flocculation performances. *Chem. Eng. J.* 349, 622–632. <https://doi.org/10.1016/j.cej.2018.05.123>
3. Almansoori, A.F., Idris, M., Abdullah, S.R.S., Anuar,

- N., Kurniawan, S.B., 2020. Response and capability of *Scirpus mucronatus* (L.) in phytotreating petrol-contaminated soil. *Chemosphere* 128760. <https://doi.org/10.1016/j.chemosphere.2020.128760>
4. Bazargan, A., Kostić, M.D., Stamenković, O.S., Veljković, V.B., McKay, G., 2015. A calcium oxide-based catalyst derived from palm kernel shell gasification residues for biodiesel production. *Fuel* 150, 519–525. <https://doi.org/10.1016/j.fuel.2015.02.046>
5. Berent, K., Komarek, S., Lach, R., Pyda, W., 2019. The effect of calcination temperature on the structure and performance of nanocrystalline mayenite powders. *Materials (Basel)*. 12. <https://doi.org/10.3390/ma12213476>
6. Boey, P.L., Maniam, G.P., Hamid, S.A., Ali, D.M.H., 2011. Utilization of waste cockle shell (*Anadara granosa*) in biodiesel production from palm olein: Optimization using response surface methodology. *Fuel* 90, 2353–2358. <https://doi.org/10.1016/j.fuel.2011.03.002>
7. Brites, C.D.S., Fiaczyk, K., Ramalho, J.F.C.B., Sójka, M., Carlos, L.D., Zych, E., 2018. Widening the Temperature Range of Luminescent Thermometers through the Intra- and Interconfigurational Transitions of Pr^{3+} . *Adv. Opt. Mater.* 6, 1701318. <https://doi.org/10.1002/adom.201701318>
8. Dümichen, E., Barthel, A.K., Braun, U., Bannick, C.G., Brand, K., Jekel, M., Senz, R., 2015. Analysis of polyethylene microplastics in environmental samples, using a thermal decomposition method. *Water Res.* 85, 451–457. <https://doi.org/10.1016/j.watres.2015.09.002>
9. Hadiyanto, H., Lestari, S.P., Abdullah, A., Widayat, W., Sutanto, H., 2016. The development of fly ash-supported CaO derived from mollusk shell of *Anadara granosa* and *Paphia undulata* as heterogeneous CaO catalyst in biodiesel synthesis. *Int. J. Energy Environ. Eng.* 7, 297–305. <https://doi.org/10.1007/s40095-016-0212-6>
10. Huang, Y.F., Lee, Y.T., Chiueh, P. Te, Lo, S.L., 2018. Microwave calcination of waste oyster shells for CO₂ capture. *Energy Procedia* 152, 1242–1247. <https://doi.org/10.1016/j.egypro.2018.09.176>
11. Imron, M.F.M.F., Kurniawan, S.B.S.B., Ismail, N., Izzati I., Abdullah, S.R.S.S.R.S., 2020. Future challenges in diesel biodegradation by bacteria isolates: A review. *J. Clean. Prod.* 251, 119716. <https://doi.org/10.1016/j.jclepro.2019.119716>
12. Kadir, A.A., Abdullah, S.R.S., Othman, B.A., Hasan, H.A., Othman, A.R., Imron, M.F., Ismail, N., Izzati, Kurniawan, S.B., 2020. Dual function of *Lemna minor* and *Azolla pinnata* as phytoremediator for Palm Oil Mill Effluent and as feedstock. *Chemosphere* 259, 127468. <https://doi.org/10.1016/j.chemosphere.2020.127468>

13. Kaewdaeng, S., Sintuya, P., Nirunsin, R., 2017. Biodiesel production using calcium oxide from river snail shell ash as catalyst. *Energy Procedia* 138, 937–942. <https://doi.org/10.1016/j.egypro.2017.10.057>
14. Kaplan, D.L., 1998. Mollusc shell structures: Novel design strategies for synthetic materials. *Curr. Opin. Solid State Mater. Sci.* 3, 232–236. [https://doi.org/10.1016/S1359-0286\(98\)80096-X](https://doi.org/10.1016/S1359-0286(98)80096-X)
15. Kouzu, M., Hidaka, J.S., 2012. Transesterification of vegetable oil into biodiesel catalyzed by CaO: A review. *Fuel* 93, 1–12. <https://doi.org/10.1016/j.fuel.2011.09.015>
16. Kurniawan, S.B., Abdullah, S.R.S., Imron, M.F., Said, N.S.M., Ismail, N., Izzati, Hasan, H.A., Othman, A.R., Purwanti, I.F., 2020. Challenges and opportunities of biocoagulant/bioflocculant application for drinking water and wastewater treatment and its potential for sludge recovery. *Int. J. Environ. Res. Public Health* 17, 1–33. <https://doi.org/10.3390/ijerph17249312>
17. Kurniawan, S.B., Imron, M.F., 2019a. The effect of tidal fluctuation on the accumulation of plastic debris in the Wonorejo River Estuary, Surabaya, Indonesia. *Environ. Technol. Innov.* 15, 100420. <https://doi.org/10.1016/j.eti.2019.100420>
18. Kurniawan, S.B., Imron, M.F., 2019b. Seasonal variation of plastic debris accumulation in the estuary of Wonorejo River, Surabaya, Indonesia. *Environ. Technol. Innov.* 16, 100490. <https://doi.org/10.1016/j.eti.2019.100490>
19. Kwon, H.B., Lee, C.W., Jun, B.S., Yun, J. Do, Weon, S.Y., Koopman, B., 2004. Recycling waste oyster shells for eutrophication control. *Resour. Conserv. Recycl.* 41, 75–82. <https://doi.org/10.1016/j.resconrec.2003.08.005>
20. Lin, S., Kiga, T., Wang, Y., Nakayama, K., 2011. Energy analysis of CaCO₃ calcination with CO₂ capture. *Energy Procedia* 4, 356–361. <https://doi.org/10.1016/j.egypro.2011.01.062>
21. Mo, K.H., Alengaram, U.J., Jumaat, M.Z., Lee, S.C., Goh, W.I., Yuen, C.W., 2018. Recycling of seashell waste in concrete: A review. *Constr. Build. Mater.* 162, 751–764. <https://doi.org/10.1016/j.conbuildmat.2017.12.009>
22. Mohamed, M., Yousuf, S., Maitra, S., 2012. Decomposition study of calcium carbonate in cockle shell. *J. Eng. Sci. Technol.*
23. Morris, J.P., Backeljau, T., Chapelle, G., 2019. Shells from aquaculture: a valuable biomaterial, not a nuisance waste product. *Rev. Aquac.* 11, 42–57. <https://doi.org/10.1111/raq.12225>
24. Nakatani, N., Takamori, H., Takeda, K., Sakugawa, H., 2009. Transesterification of soybean oil using combusted oyster shell waste as a catalyst. *Bioresour. Technol.* 100, 1510–1513. <https://doi.org/10.1016/j.biortech.2008.09.007>
25. Nordin, N., Hamzah, Z., Hashim, O., Kasim, F.H., Abdullah, R., 2015. Effect of temperature in calcination process of seashells. *Malaysian J. Anal. Sci.*
26. Purwanti, I.F., Kurniawan, S.B., Tangahu, B.V., Rahayu, N.M., 2017. Bioremediation of trivalent chromium in soil using bacteria. *Int. J. Appl. Eng. Res.* 12, 9346–9350.
27. Raizada, P., Shandilya, P., Singh, P., Thakur, P., 2017. Solar light-facilitated oxytetracycline removal from the aqueous phase utilizing a H₂O₂/ZnWO₄/CaO catalytic system. *J. Taibah Univ. Sci.* 11, 689–699. <https://doi.org/10.1016/j.jtusci.2016.06.004>
28. Ramasamy, K.K., Gray, M., Job, H., Santosa, D., Li, X.S., Devaraj, A., Karkamkar, A., Wang, Y., 2016. Role of Calcination Temperature on the Hydrotalcite Derived MgO-Al₂O₃ in Converting Ethanol to Butanol. *Top. Catal.* 59, 46–54. <https://doi.org/10.1007/s11244-015-0504-8>
29. Saleh, T.A., Tuzen, M., Sari, A., 2017. Magnetic activated carbon loaded with tungsten oxide nanoparticles for aluminum removal from waters. *J. Environ. Chem. Eng.* 5, 2853–2860. <https://doi.org/10.1016/j.jece.2017.05.038>
30. Sirisomboonchai, S., Abuduwayiti, M., Guan, G., Samart, C., Abliz, S., Hao, X., Kusakabe, K., Abudula, A., 2015. Biodiesel production from waste cooking oil using calcined scallop shell as catalyst. *Energy Convers. Manag.* 95, 242–247. <https://doi.org/10.1016/j.enconman.2015.02.044>
31. Suryaputra, W., Winata, I., Indraswati, N., Ismadji, S., 2013. Waste capiz (*Amusium cristatum*) shell as a new heterogeneous catalyst for biodiesel production. *Renew. Energy* 50, 795–799. <https://doi.org/10.1016/j.renene.2012.08.060>
32. Tang, Y., Chen, G., Zhang, J., Lu, Y., 2011. Highly active cao for the transesterification to biodiesel production from rapeseed oil. *Bull. Chem. Soc. Ethiop.* 25, 37–42. <https://doi.org/10.4314/bcse.v25i1.63359>
33. Titah, H.S., Pratikno, H., Moesriati, A., Imron, M.F., Putera, R.I., 2018a. Isolation and screening of diesel degrading bacteria from ship dismantling facility at Tanjungjati, Madura, Indonesia. *J. Eng. Technol. Sci.* 50, 99. <https://doi.org/10.5614/j.eng.technol.sci.2018.50.1.7>
34. Titah, H.S., Purwanti, I.F., Tangahu, B.V., Kurniawan, S.B., Imron, M.F., Abdullah, S.R.S., Ismail, N., Izzati, 2019. Kinetics of aluminium removal by locally isolated *Brochothrix thermosphacta* and *Vibrio alginolyticus*. *J. Environ. Manage.* 238, 194–200. <https://doi.org/10.1016/j.jenvman.2019.03.011>
35. Titah, H.S., Rozaimah, S., Abdullah, S.R.S., Idris, M., Anuar, N., Basri, H., Mukhlisin, M., Tangahu, B.V., Purwanti, I.F., Kurniawan, S.B., 2018b. Arsenic resistance and biosorption by isolated *Rhizobacteria* from the roots of *Ludwigia*

- octovalvis. *Int. J. Microbiol.* 2018, 1–10. <https://doi.org/10.1155/2018/3101498>
36. Wang, G., Dai, J., Luo, Q., Deng, N., 2021. Photocatalytic degradation of bisphenol A by TiO₂@aspartic acid-β-cyclodextrin@reduced graphene oxide. *Sep. Purif. Technol.* <https://doi.org/10.1016/j.seppur.2020.117574>
37. Wang, J., Liu, E., Li, L., 2019. Characterization on the recycling of waste seashells with Portland cement towards sustainable cementitious materials. *J. Clean. Prod.* 220, 235–252. <https://doi.org/10.1016/j.jclepro.2019.02.122>
38. Wang, W., Lin, F., Yan, B., Cheng, Z., Chen, G., Kuang, M., Yang, C., Hou, L., 2020. The role of seashell wastes in TiO₂/Seashell composites: Photocatalytic degradation of methylene blue dye under sunlight. *Environ. Res.* 188, 109831. <https://doi.org/10.1016/j.envres.2020.109831>
39. Wulandari, K.D., Ekaputri, J.J., Triwulan, Kurniawan, S.B., Primaningtyas, W.E., Abdullah, S.R.S., Ismail, N., ‘Izzati, Imron, M.F., 2021. Effect of microbes addition on the properties and surface morphology of fly ash-based geopolymer paste. *J. Build. Eng.* 33. <https://doi.org/10.1016/j.jobbe.2020.101596>
40. Yoon, G.L., Kim, B.T., Kim, B.O., Han, S.H., 2003. Chemical-mechanical characteristics of crushed oyster-shell. *Waste Manag.* 23, 825–834. [https://doi.org/10.1016/S0956-053X\(02\)00159-9](https://doi.org/10.1016/S0956-053X(02)00159-9)